BULLETIN OF THE POLISH ACADEMY OF SCIENCES
TECHNICAL SCIENCES, Vol. 69(3), 2021, Article number: e137056
DOI: 10.24425/bpasts.2021.137056

Hybrid synchronization and parameter estimation of a complex chaotic network of permanent magnet synchronous motors using adaptive integral sliding mode control

Nazam SIDDIQUE* and Fazal U. REHMAN

Capital University of Science and Technology, Islamabad Expressway, Kahuta Road, Zone-V Islamabad, Pakistan

Abstract. The synchronisation of a complex chaotic network of permanent magnet synchronous motor systems has increasing practical importance in the field of electrical engineering. This article presents the control design method for the hybrid synchronization and parameter estimation of ring-connected complex chaotic network of permanent magnet synchronous motor systems. The design of the desired control law is a challenging task for control engineers due to parametric uncertainties and chaotic responses to some specific parameter values. Controllers are designed based on the adaptive integral sliding mode control to ensure hybrid synchronization and estimation of uncertain terms. To apply the adaptive ISMC, firstly the error system is converted to a unique system consisting of a nominal part along with the unknown terms which are computed adaptively. The stabilizing controller incorporating nominal control and compensator control is designed for the error system. The compensator controller, as well as the adopted laws, are designed to get the first derivative of the Lyapunov equation strictly negative. To give an illustration, the proposed technique is applied to 4-coupled motor systems yielding the convergence of error dynamics to zero, estimation of uncertain parameters, and hybrid synchronization of system states. The usefulness of the proposed method has also been tested through computer simulations and found to be valid.

Key words: chaotic system; hybrid synchronization (HS); complex chaotic permanent magnet synchronous motor; adaptive integral sliding mode control (ISMC); Lyapunov function.

1. Introduction

Since the pioneering work by A.C. Fowler et al. [1], complex chaotic systems have become an interesting field of research over the last few decades, especially synchronization of complex natured chaotic systems have attracted the attention of many researchers. Complex systems have a broad range of applications in industrial areas and it is very important to understand numerous physical systems like a chaotic complex system. Synchronization of complex chaotic systems is a fascinating subject, especially in communications [2–5]. Synchronization methods used for simple chaotic systems are extended for complex systems like lag synchronization [6], anti-synchronization [7], adaptive anti-synchronization for unknown parameters [8], hybrid synchronization (HS) and parameter identification of chaotic systems coupled in ring topology [9] and projective synchronization [10]. In addition, there are some other techniques reported in the literature [11–17], which were designed particularly for complex chaotic systems.

All the techniques mentioned above are mainly designed for synchronization of two or more [18] complex systems, where one is usually the drive system and the other is the response system. The purpose of these kinds of techniques was that the states of the response system follow the trajectories of drive systems. Instead of using simple techniques, the synchronization technique for multiple coupled complex chaotic systems can improve the protection of message signals in secure communication and it also has a bright future in the communication field. Consequently, many researchers are attracted to this field of research and are making their efforts to analyze multiple coupled systems. Wang et al. [19] evaluated adaptive combination synchronization of complex and real dynamical systems. Zhou et al. [20] investigated adaptive synchronization for uncertain complex networks.

The hybrid synchronization (HS) of multiple coupled complex dynamical systems was reported in [21], where synchronization/anti-synchronization are achieved for complex systems connected in the ring topology and with known parameters. A ring topology is shown in Fig. 1, where the states of first system track the states of N-th system, states of the second follow the states of the first complex chaotic systems and so on, finally the states of the last system follow the states of $(N-1)$-th complex chaotic system. Synchronization and anti-synchronization for real chaotic systems coupled in the ring

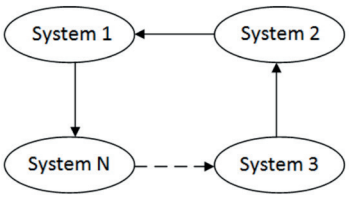

Fig. 1. Ring topology

*e-mail: nazim.siddiq@gmail.com

Manuscript submitted 2020-09-29, revised 2021-02-12, initially accepted for publication 2021-03-01, published in June 2021

topology are achieved in [21], but complex systems connected in the ring topology is a less focused area of research.

Several different methods were reported in the literature [21, 22] for chaotic synchronization. The active control technique is a significant and easy control method because it provides a convenient way to select and implement the controllers. In an active control technique, the controllers are selected to nullify the nonlinear terms, which are present in the system, therefore, chaotic synchronization becomes a linear problem. The direct design control method is investigated in [23]. Meanwhile, the sliding mode control (SMC) [24] is a bit difficult approach. However, it has a lot of advantages, like the fast response and robustness in opposition to the parameter deviation and external disturbances.

A modification of SMC technique is the integral sliding mode control (ISMC) [25] which combines the discontinuous control and nominal control. The main advantage of applying the ISMC is that it eliminates the reaching phase. So, robustness is guaranteed throughout the system response.

Medium power permanent magnet synchronous motors (PMSM) are very useful in industrial applications due to their significant features like a small size, low cost, and high torque. Especially, the simple structure of PMSM, in which there is no field winding present in the motor, makes it first choice for the industrial applications. Therefore, a lot of research has been conducted to investigate control and synchronization of real permanent magnet synchronous motors [26–28], whereas much less work is being done for complex variable permanent magnet synchronous motors [29]. Recently, some new results related to the control of PMSM were documented in [30–32]. Practically, in PMSM, complex currents and complex voltages are present in the dynamical model and there is a possibility that one or all the parameters of the systems are disturbed due to noise. So, it is practically sound to estimate the unknown parameters for HS of PMSM systems. In this research, an effort has been made to reach HS and identification of uncertain parameters for a complex chaotic network of PMSM systems connected in the ring topology.

2. System description

In [33] the mathematical model of a field-oriented PMSM rotor system is given as:

$$\begin{aligned}\frac{di_d}{dt} &= \frac{(-R_1 i_d + w i_q L_q + u_d)}{L_d},\\ \frac{di_q}{dt} &= \frac{(-R_1 i_q + w i_d L_d - w\psi_r + u_q)}{L_q},\\ \frac{dw}{dt} &= \frac{(n_p \psi_r i_q + n_p i_d i_q (L_d - L_q) - w\beta - T_L)}{J}.\end{aligned} \tag{1}$$

According to this mathematical model (1) the dynamic state variables i_q, i_d represent currents and w is angular frequency; u_d is the direct axis and u_q is the quadrature-axis component of input stator voltages; T_L is the applied load torque; J is the arctic moment of inertia; R_1 represents resistance of stator wingding; β is the adhesive damping constant; L_d represents direct axis inductance and L_q represents quadrature-axis inductance; ψ_r represents rotor flux and n_p are the total number of rotor poles. When there is an even air gap, uniform flux distribution, and the motor operates at no-load, the mathematical model of PMSM can simply be presented as:

$$\begin{aligned}\dot{x_1} &= (x_2 - x_1)(a),\\ \dot{x_2} &= b x_1 - x_2 - x_1 x_3,\\ \dot{x_3} &= x_1 x_2 - x_3.\end{aligned} \tag{2}$$

This system has two complex variables x_1, x_2 and two constant parameters a, b. In [22] another complex model of permanent magnet synchronous motor is presented as:

$$\begin{aligned}\dot{x_1} &= (x_2 - x_1)(a),\\ \dot{x_2} &= b x_1 - x_1 x_3 - x_2,\\ \dot{x_3} &= 0.5(x_2 \overline{x_1} + \overline{x_2} x_1),\end{aligned} \tag{3}$$

where $\overline{x_1}$, $\overline{x_2}$ are in complex conjugate form with $j = \sqrt{-1}$. This system shows chaotic behavior when its constant parameters are selected as $b = 20, a = 11$. Figures 2(a)–2(b), depict the chaotic behavior of this system. There are many properties of PMSM systems studied in [34]. In this research paper, we are examining parameter identification and HS of PMSM systems using adaptive ISMC.

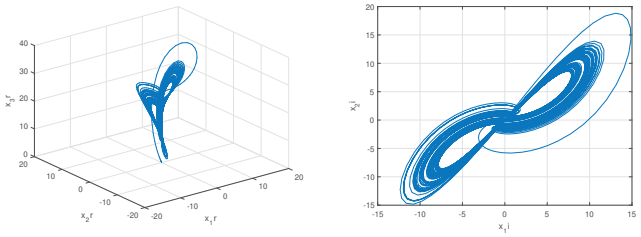

(a) (b)

Fig. 2. (a) Chaotic behaviour of PMSM system on x_{1r}, x_{2r}, x_{3r} space, (b) Chaotic behaviour of PMSM system on x_{1i}, x_{2i} space

The remaining paper is organized as: in Section 3, HS control problem formulation. In Section 4, the proposed control algorithm is discussed where as, in Section 5, HS for PMSM systems is discussed. In Section 6, simulation results are discussed and in Section 7, the paper is concluded.

3. HS control problem formulation

In general, N complex chaotic systems connected in a ring topology can be configured as:

$$\begin{aligned}\dot{x}_1 &= f_1(x_1) + F_1(x_1)\theta_1 + D_1(x_N - x_1),\\ \dot{x}_2 &= f_2(x_2) + F_2(x_2)\theta_2 + D_2(x_1 - x_2),\\ &\vdots\\ \dot{x}_N &= f_N(x_N) + F_N(x_N)\theta_N + D_N(x_{N-1} - x_N),\end{aligned} \tag{4}$$

where $x_1, x_2, ..., x_N \in C^n$, are defined as the complex state vectors, $x_i = (x_{i1}, x_{i2}, x_{i3}, ..., x_{in})^T$, $x_k = x_{kr} + jx_{ki}, k = 1,2,3,...,N$, $j = \sqrt{-1}$, both subscripts r and i represent real as well as imaginary components from the beginning to the end of this paper, $f_i : C^n \to C^n$ are the continuous nonlinear function, $\theta_i \in \Re^p$ are unknown parameters, $F_i(x_i) \in C^(n \times p)$ are matrices, $D_i = diag\{d_{i1}, d_{i2}, d_{i3}..., d_{iN}\}, i = 1,2,3,...,N$ are N-dimensional diagonal matrices, as well as $d_{ij} \geq 0$ represents connected terms of D_i. In Fig. 1, the complex chaotic dynamic systems are connected in a ring, in which the dynamic states of the 1st system couples the Nth, the 2^{nd} system couples the 1st, so on, and finally, the N-th complex chaotic system couples the $(N-1)$-th.

The network model presented in (4) is very practical and unique in the sense that it contains unknown constant terms θ_i. The constant terms of (4) are assumed to be uncertain due to noise or some other unwanted external disturbances. The uncertain terms will be estimated by the proposed control algorithm. In this research, we have utilized this coupling scheme to investigate HS and it can be mathematically represented as:

$$\begin{aligned} \dot{x}_1 &= f_1(x_1) + F_1(x_1)\theta_1 + D_1(x_N - x_1), \\ \dot{x}_2 &= f_2(x_2) + F_2(x_2)\theta_2 + D_2(x_1 - x_2) + u_1, \\ &\vdots \\ \dot{x}_N &= f(x_N) + F_N(x_N)\theta_N + D_N(x_{N-1} - x_N) + u_{N-1}, \end{aligned} \tag{5}$$

where $u_k = u_{kr} + ju_{ki}, k = 1,2,...,N-1$ are the complex inputs. The hybrid synchronization for multiple connected system is defined as:

Definition 1. The chaotic dynamic system (5), we say, there exists hybrid synchronization conceding that the controllers u_i, $i = 1,2,3,...,N-1$ are selected in such a manner that all the trajectories $x_1(t), x_2(t), ..., x_N(t))$ in (5) with either initial conditions $(x_1(0), x_2(0), ..., x_N(0))$ satisfy: For the errors $e_i = (e_{i1}, e_{i2}, ..., e_{iN})^T$, we have

$$\lim_{t\to\infty} e_i = \lim_{t\to\infty} x_i(t) + qx_{i+1}(t) = 0, \quad i = 1,2,3,...,N-1.$$

For the anti-synchronization we choose $q = 1$ and for complete synchronization $q = -1$. The problem of hybrid synchronization can be resolved by designing appropriate controllers u_i to get $e_i = (e_{i1}, e_{i2}, ..., e_{iN})^T \to 0$ asymptotically.

4. The proposed control algorithm

For the hybrid synchronization, we define the error vectors as:

$$\begin{aligned} e_1 &= x_2 + qx_1, \\ e_2 &= x_3 + qx_2, \\ &\vdots \\ e_{N-1} &= x_N + qx_{N-1}. \end{aligned} \tag{6}$$

Let $\hat{\theta}_i$ be the estimate of θ_i and let $\tilde{\theta}_i = \theta_i - \hat{\theta}_i$ be the errors in estimating the parameters $\theta_i, i = 1,2,\cdots,N$, respectively. The first derivative of (6) yields the following:

$$\begin{bmatrix} \dot{e}_1 \\ \dot{e}_2 \\ \dot{e}_3 \\ \vdots \\ \dot{e}_{N-1} \end{bmatrix} = \begin{bmatrix} f_2(x_2) + qf_1(x_1) + F_2(x_2)\hat{\theta}_2 + qF_1(x_1)\hat{\theta}_1 \\ +D_2(x_1 - x_2) + qD_1(x_N - x_1) \\ f_3(x_3) + qf_2(x_2) + F_3(x_3)\hat{\theta}_3 + qF_2(x_2)\hat{\theta}_2 \\ +D_3(x_2 - x_3) + qD_2(x_1 - x_2) \\ f_4(x_4) + qf_3(x_3) + F_4(x_4)\hat{\theta}_4 + qF_3(x_3)\hat{\theta}_3 \\ +D_4(x_3 - x_4) + qD_3(x_2 - x_3) \\ \vdots \\ f_N(x_N) + qf_{N-1}(x_{N-1}) + F_N(x_N)\hat{\theta}_N \\ +qF_{N-1}(x_{N-1})\hat{\theta}_{N-1} + D_N(x_{N-1} - x_N) \\ +qD_{N-1}(x_{N-2} - x_{N-1}) \end{bmatrix}$$

$$+ \begin{bmatrix} F_2(x_2)\tilde{\theta}_2 + qF_1(x_1\tilde{\theta}_1) \\ F_3(x_3)\tilde{\theta}_3 + qF_2(x_2\tilde{\theta}_2) \\ F_4(x_4)\tilde{\theta}_4 + qF_3(x_3\tilde{\theta}_3) \\ \vdots \\ F_N(x_N)\tilde{\theta}_N \\ +qF_{N-1}(x_{N-1}\tilde{\theta}_{N-1}) \end{bmatrix} + \begin{bmatrix} 1 & 0 & 0 & \cdots & 0 \\ q & 1 & 0 & \cdots & 0 \\ 0 & q & 1 & \cdots & 0 \\ \vdots & \vdots & \vdots & \vdots & \vdots \\ 0 & 0 & \cdots & q & 1 \end{bmatrix} \begin{bmatrix} u_1 \\ u_2 \\ \vdots \\ u_{N-1} \end{bmatrix}. \tag{7}$$

By choosing:

$$\begin{bmatrix} u_1 \\ u_2 \\ \vdots \\ u_{N-1} \end{bmatrix} = \begin{bmatrix} 1 & 0 & 0 & \cdots & 0 \\ q & 1 & 0 & \cdots & 0 \\ 0 & q & 1 & \cdots & 0 \\ \vdots & \vdots & \vdots & \vdots & \vdots \\ 0 & 0 & \cdots & q & 1 \end{bmatrix}^{-1} \left\{ + \begin{bmatrix} e_2 \\ e_3 \\ \vdots \\ e_{N-1} \\ v \end{bmatrix} - A \right\} \tag{8}$$

where, v is the new input vector and

$$A = \begin{bmatrix} f_2(x_2) + qf_1(x_1) + F_2(x_2)\hat{\theta}_2 + qF_1(x_1)\hat{\theta}_1 \\ +D_2(x_1 - x_2) + qD_1(x_N - x_1) \\ f_3(x_3) + qf_2(x_2) + F_3(x_3)\hat{\theta}_3 + qF_2(x_2)\hat{\theta}_2 \\ +D_3(x_2 - x_3) + qD_2(x_1 - x_2) \\ f_4(x_4) + qf_3(x_3) + F_4(x_4)\hat{\theta}_4 + qF_3(x_3)\hat{\theta}_3 \\ +D_4(x_3 - x_4) + qD_3(x_2 - x_3) \\ \vdots \\ f_N(x_N) + qf_{N-1}(x_{N-1}) + F_N(x_N)\hat{\theta}_N \\ +qF_{N-1}(x_{N-1})\hat{\theta}_{N-1} + D_N(x_{N-1} - x_N) \\ +qD_{N-1}(x_{N-2} - x_{N-1}) \end{bmatrix}. \tag{9}$$

and replacing (8) in (7) the error dynamic system presented in (7) becomes as:

$$\begin{aligned} \dot{e}_1 &= e_2 + F_2(x_2)\tilde{\theta}_2 + qF_1(x_1)\tilde{\theta}_1, \\ \dot{e}_2 &= e_3 + F_3(x_3)\tilde{\theta}_3 + qF_2(x_2)\tilde{\theta}_2, \\ \dot{e}_3 &= e_4 + F_4(x_4)\tilde{\theta}_4 + qF_3(x_3)\tilde{\theta}_3, \\ &\vdots \\ \dot{e}_{N-2} &= e_{N-1} + F_{N-1}(x_{N-1})\tilde{\theta}_{N-1} + qF_{N-2}(x_{N-2})\tilde{\theta}_{N-2}, \\ \dot{e}_{N-1} &= v + F_N(x_N)\tilde{\theta}_N + qF_{N-1}(x_{N-1})\tilde{\theta}_{N-1}. \end{aligned} \tag{10}$$

To apply the ISMC, firstly we have to define the nominal system for (10):

$$\begin{aligned} \dot{e}_1 &= e_2\,, \\ \dot{e}_2 &= e_3\,, \\ \dot{e}_3 &= e_4\,, \\ &\vdots \\ \dot{e}_{N-2} &= e_{N-1}\,, \\ \dot{e}_{N-1} &= v_o\,. \end{aligned} \tag{11}$$

To stabilize the error system in (11), the Hurwitz sliding surface is designed as: $\sigma_o = (1+\frac{d}{dt})^{N-2}e_1 = e_1 + c_1e_2 + ... + c_{N-3}e_{N-1}$, where the coefficients c_i are chosen in such a way that σ_o becomes Hurwitz polynomial. The time derivative of the above sliding surface will be like this $\dot{\sigma}_o = e_2 + c_1e_3 + c_2e_4 + ... + c_{N-3}e_{N-1} + v_o$. By choosing $v_o = -e_2 - c_1e_3 - c_2e_4 - ... - c_{N-3}e_{N-1} - k\sigma_o, k > 0$, we have $\dot{\sigma}_o = -k\sigma_o$, consequently $\sigma_o \to 0$, which gives $e_1, e_2, ..., e_{N-1} \to 0$. In consequence system (11) is asymptotically stable. Moreover, by designing sliding surfaces for the above system (10) as: $\sigma = \sigma_o + z$ where z in this equation is an integral parameter which shall be computed subsequently. To avert reaching phase set $z(0)$ such that $\sigma(0) = 0$. The time derivative of this sliding manifold will be as following:

$$\begin{aligned} \dot{\sigma} &= \dot{\sigma}_o + \dot{z} \\ &= \dot{e}_1 + c_1\dot{e}_2 + ... + c_{N-3}\dot{e}_{N-2} + \dot{e}_{N-1} + v + \dot{z} \\ &= e_2 + \sum_{i=3}^{N-1} c_{i-2}e_i + v + \dot{z} + qF_1(x_1)\tilde{\theta}_1 \\ &\quad + \left((1+qc_1)F_2(x_2)\tilde{\theta}_2\right) \\ &\quad + \sum_{i=1}^{N-4}(c_i + qc_{i+1})F_{i+2}(x_{i+2})\tilde{\theta}_{i+2} \\ &\quad + \left((c_{N-3}+q)F_{N-1}(x_{N-1})\tilde{\theta}_{N-1}\right) + F_N(x_N)\tilde{\theta}_N\,. \end{aligned} \tag{12}$$

The new input term v in (12) is defined as $v = v_s + v_0$, where v_0 is the nominal input vector and the other term v_s is a compensator input vector which will be computed later. The Lyapunov stability function for (12) is defined as:

$$\begin{aligned} V = \frac{1}{2}\Big\{ &\sigma^T\sigma + \tilde{\theta}_1^T\tilde{\theta}_1 + \tilde{\theta}_2^T\tilde{\theta}_2 + \sum_{i=1}^{N-4}\tilde{\theta}_{i+2}^T\tilde{\theta}_{i+2} \\ &+ \tilde{\theta}_{N-1}^T\tilde{\theta}_{N-1} + \tilde{\theta}_N^T\tilde{\theta}_N\Big\} \end{aligned} \tag{13}$$

by properly defining the adaptive laws $\tilde{\theta}_i$, $\hat{\theta}_i$, $i = 1,2,3,...,N$, and computing the compensator input vector v_s such that the fist derivative of (13) can be achieved as $\dot{V} < 0$.

Theorem 1. For the Lyapunov equation as described in (13) it is possible to get $\dot{V} < 0$ conceding that $\tilde{\theta}_i$, $\hat{\theta}_i$, $i = 1,2,3,...,N$ and v_s are chosen as:

$$\begin{aligned} \dot{z} &= -e_2 - \sum_{i=3}^{N-1} c_{i-2}e_i - v_o, \\ v_s &= -k\sigma - ksign(\sigma), \\ \dot{\tilde{\theta}}_1 &= -qF_1^T(x_1)\sigma - k_1\tilde{\theta}_1, \\ \dot{\hat{\theta}}_1 &= -\dot{\tilde{\theta}}_1\,, \\ \dot{\tilde{\theta}}_2 &= -(1+qc_1)F_2^T(x_2)\sigma - k_2\tilde{\theta}_2, \\ \dot{\hat{\theta}}_2 &= -\dot{\tilde{\theta}}_2\,, \\ \dot{\tilde{\theta}}_{i+2} &= -(c_i + qc_{i+1})F_{i+1}^T(x_{i+2})\sigma - k_{N-1} - k_{i+2}\tilde{\theta}_{i+2}, \\ \dot{\hat{\theta}}_{i+2} &= -\dot{\hat{\theta}}_{i+2}, \qquad i = 1,...,N-4, \\ \dot{\tilde{\theta}}_{N-1} &= -(c_{N-3}+q)F6T_{N-1}\sigma - k_{N-1}\tilde{\theta}_{N-1}, \\ \dot{\hat{\theta}}_{N-1} &= -\dot{\tilde{\theta}}_{N-1}, \\ \dot{\tilde{\theta}}_N &= -F_N^T(x_N)\sigma - k_N\tilde{\theta}_N, \\ \dot{\hat{\theta}}_N c &= -\dot{\tilde{\theta}}_N\,. \end{aligned} \tag{14}$$

Proof. Since:

$$\begin{aligned} \dot{V} &= \sigma^T\dot{\sigma} + \tilde{\theta}_1^T\dot{\tilde{\theta}}_1 + \tilde{\theta}_2^T\dot{\tilde{\theta}}_2 \\ &\quad + \sum_{i=1}^{N-4}\tilde{\theta}_{i+2}^T\dot{\tilde{\theta}}_{i+2} + \tilde{\theta}_{N-1}^T\dot{\tilde{\theta}}_{N-1} + \tilde{\theta}_N^T\dot{\tilde{\theta}}_N \\ &= \sigma^T\left\{e_2 + \sum_{i=3}^{N-1}c_{i-2}e_i + v_o + v_s + \dot{z}\right\} + \tilde{\theta}_1^T\left\{\dot{\tilde{\theta}}_1 + qFF_1^T(x_1)\sigma\right\} \\ &\quad + \tilde{\theta}_2^T\left\{\dot{\tilde{\theta}}_2 + (1+qc_1)F_2^T(x_2)\sigma\right\} \\ &\quad + \sum_{i=1}^{N-4}\tilde{\theta}_{i+2}^T\left\{\dot{\tilde{\theta}}_{i+2} + (c_i + qc_{i+1})F_{i+2}^T(x_{i+2})\sigma\right\} \\ &\quad + \tilde{\theta}_{N-1}^T\left\{\dot{\tilde{\theta}}_{N-1} + (c_{N-3}+q)F_{N-1}^T(x_{N-1})\sigma\right\} \\ &\quad + \tilde{\theta}_N^T\left\{\dot{\tilde{\theta}}_N + F_N^T(x_N)\sigma\right\}. \end{aligned} \tag{15}$$

By replacing (14) in (15) we get:

$$\dot{V} = -k\sigma^2 - \sum_{i=1}^{N} k_i\tilde{\theta}_i^T\tilde{\theta}_i - k\sigma^T sign(\sigma), \quad k > 0. \tag{16}$$

This shows σ and $\tilde{\theta}_i \to 0$ consequently $e_i \to 0$, $i = 1,2,3,..,N-1$.

5. HS of ring-connected complex PMSM systems

In this section, we investigate HS of N-coupled complex PMSM systems connected in ring topology. Assuming $N = 4$, the coupled complex PMSM systems in a ring topology can be represented as:

$$
\begin{aligned}
\dot{x}_{11} &= a(x_{12}-x_{11})+d_{11}(x_{41}-x_{11}),\\
\dot{x}_{12} &= bx_{11}-x_{12}-x_{11}x_{13}+d_{12}(x_{42}-x_{12}),\\
\dot{x}_{13} &= 0.5(\bar{x}_{11}x_{12}+x_{11}\bar{x}_{12})-x_{13}+d_{13}(x_{43}-x_{13}),\\
\dot{x}_{21} &= a(x_{22}-x_{21})+d_{21}(x_{11}-x_{21})+\mu_{11},\\
\dot{x}_{22} &= bx_{21}-x_{22}-x_{21}x_{23}+d_{22}(x_{12}-x_{22})+\mu_{12},\\
\dot{x}_{23} &= 0.5(\bar{x}_{21}x_{22}+x_{21}\bar{x}_{22})-x_{23}+d_{23}(x_{13}-x_{23})+\mu_{13},\\
\dot{x}_{31} &= a(x_{32}-x_{31})+d_{31}(x_{21}-x_{31})+\mu_{21},\\
\dot{x}_{32} &= bx_{31}-x_{32}-x_{31}x_{33}+d_{32}(x_{22}-x_{32})+\mu_{22},\\
\dot{x}_{33} &= 0.5(\bar{x}_{31}x_{32}+x_{31}\bar{x}_{32})-x_{33}+d_{33}(x_{23}-x_{33})+\mu_{23},\\
\dot{x}_{41} &= a(x_{42}-x_{41})+d_{41}(x_{31}-x_{41})+\mu_{31},\\
\dot{x}_{42} &= bx_{41}-x_{42}-x_{41}x_{43}+d_{42}(x_{32}-x_{42})+\mu_{32},\\
\dot{x}_{43} &= 0.5(\bar{x}_{41}x_{42}+x_{41}\bar{x}_{42})-x_{43}+d_{33}(x_{33}-x_{43})+\mu_{33},
\end{aligned}
\tag{17}
$$

where, $x_{k1}=x_{k1r}+jx_{k1i}$, $x_{k2}=x_{k2r}+jx_{k2i}$ are complex and $x_{k3}=x_{k3r}$ are real, $\bar{x}_{k1}$, $\bar{x}_{k2}$ denote the complex conjugate variables of x_{k1}, x_{k2}, $k=1,2,3,4$ and a, b are unknown real terms.

In (17), if the paramaters a and b are uncertain and their estimates are $\hat{a}$ and $\hat{b}$ respectively, the error in estimation of uncertain parameters can be described as: $\tilde{a}=a-\hat{a}$, $\tilde{b}=b-\hat{b}$, then (17) can be written in vector form as:

$$
\begin{aligned}
\dot{x}_{1r} &= f_{1r}+F_{1r}\hat{\theta}+F_{1r}\tilde{\theta}+D_1G_{1r},\\
\dot{x}_{1i} &= f_{1i}+F_{1i}\hat{\theta}+F_{1i}\tilde{\theta}+D_1G_{1i},\\
\dot{x}_{2r} &= f_{2r}+F_{2r}\hat{\theta}+F_{2r}\tilde{\theta}+D_2G_{2r}+\mu_{1r},\\
\dot{x}_{2i} &= f_{2i}+F_{2i}\hat{\theta}+F_{2i}\tilde{\theta}+D_2G_{2i}+\mu_{1i},\\
\dot{x}_{3r} &= f_{3r}+F_{3r}\hat{\theta}+F_{3r}\tilde{\theta}+D_3G_{3r}+\mu_{2r},\\
\dot{x}_{3i} &= f_{3i}+F_{3i}\hat{\theta}+F_{3i}\tilde{\theta}+D_3G_{3i}+\mu_{2i},\\
\dot{x}_{4r} &= f_{4r}+F_{4r}\hat{\theta}+F_{4r}\tilde{\theta}+D_4G_{4r}+\mu_{3r},\\
\dot{x}_{4i} &= f_{4i}+F_{4i}\hat{\theta}+F_{4i}\tilde{\theta}+D_3G_{4i}+\mu_{3i},
\end{aligned}
\tag{18}
$$

where

$$
\begin{aligned}
f_{kr} &= \begin{bmatrix} 0 \\ -x_{k2r}-x_{k1r}x_{k3} \\ 0.5(x_{k1r}x_{k2r}+x_{k1i}x_{k2i})-x_{k3} \end{bmatrix},\\
f_{ki} &= \begin{bmatrix} 0 \\ -x_{k2r}-x_{k1r}x_{k3} \\ 0 \end{bmatrix}, \quad k=1,2,3,4;\\
F_{kr} &= \begin{bmatrix} x_{k2r}-x_{k1r} & 0 \\ 0 & x_{k1r} \\ 0 & 0 \end{bmatrix},\\
F_{ki} &= \begin{bmatrix} x_{k2i}-x_{k1i} & 0 \\ 0 & x_{k1i} \\ 0 & 0 \end{bmatrix},
\end{aligned}
\tag{19}
$$

$$
\begin{aligned}
G_{1r} &= \begin{bmatrix} x_{41r}-x_{11r} \\ x_{42r}-x_{12r} \\ x_{4r}-x_{13} \end{bmatrix}, \quad G_{1i} = \begin{bmatrix} x_{41i}-x_{11i} \\ x_{42i}-x_{12i} \\ 0 \end{bmatrix},\\
G_{2r} &= \begin{bmatrix} x_{11r}-x_{21r} \\ x_{12r}-x_{22r} \\ x_{13}-x_{43} \end{bmatrix}, \quad G_{2i} = \begin{bmatrix} x_{11i}-x_{21i} \\ x_{12i}-x_{22i} \\ 0 \end{bmatrix},\\
G_{3r} &= \begin{bmatrix} x_{21r}-x_{31r} \\ x_{22r}-x_{32r} \\ x_{23}-x_{33} \end{bmatrix}, \quad G_{3i} = \begin{bmatrix} x_{21i}-x_{31i} \\ x_{22i}-x_{32i} \\ 0 \end{bmatrix},\\
G_{4r} &= \begin{bmatrix} x_{31r}-x_{41r} \\ x_{32r}-x_{42r} \\ x_{33}-x_{43} \end{bmatrix}, \quad G_{4i} = \begin{bmatrix} x_{31i}-x_{41i} \\ x_{32i}-x_{42i} \\ x_{33}-x_{43} \end{bmatrix},\\
u_{lr} &= \begin{bmatrix} u_{l1r} \\ u_{l2r} \\ u_{lr} \end{bmatrix}, \quad u_{li} = \begin{bmatrix} u_{l1i} \\ u_{l2i} \\ 0 \end{bmatrix}, \quad l=1,2,3,\\
\hat{\theta} &= \begin{bmatrix} \hat{a} \\ \hat{b} \end{bmatrix}, \quad \tilde{\theta} = \begin{bmatrix} \tilde{a} \\ \tilde{b} \end{bmatrix}.
\end{aligned}
\tag{19}
$$

Defining the error as: $e_k = e_{kr}+je_{ki} = x_{k+1}+qx_k = x_{(k+1)r}+qx_{kr}+jx_{(k+1)i}+qx_{ki}$, this gives $e_{kr}=x_{(k+1)r}+qx_{kr}$ and, $e_{ki}=x_{(k+1)i}+qx_{ki}$, $k=1,2,3$. The error dynamics of this system becomes as:

$$
\begin{aligned}
\begin{bmatrix} \dot{e}_{1r} \\ \dot{e}_{2r} \\ \dot{e}_{3r} \end{bmatrix} &= \begin{bmatrix} (f_{2r}+qf_{1r})+(F_{2r}+qF_{1r}\hat{\theta})+D_2G_{2r}+qD_1G_{1r}) \\ (f_{3r}+qf_{2r})+(F_{3r}+qF_{2r}\hat{\theta})+D_3G_{3r}+qD_2G_{2r}) \\ (f_{4r}+qf_{3r})+(F_{4r}+qF_{3r}\hat{\theta})+D_4G_{4r}+qD_3G_{3r}) \end{bmatrix}\\
&+ \begin{bmatrix} F_{2r}+qF_{1r} \\ F_{3r}+qF_{2r} \\ F_{4r}+qF_{3r} \end{bmatrix} + \begin{bmatrix} I & 0 & 0 \\ -qI & I & 0 \\ 0 & -qI & I \end{bmatrix} \begin{bmatrix} \mu_{1r} \\ \mu_{2r} \\ \mu_{3r} \end{bmatrix},\\
\begin{bmatrix} \dot{e}_{1i} \\ \dot{e}_{2i} \\ \dot{e}_{3i} \end{bmatrix} &= \begin{bmatrix} (f_{2i}+qf_{1i})+(F_{2i}+qF_{1i}\hat{\theta})+D_2G_{2i}+qD_1G_{1i}) \\ (f_{3i}+qf_{2i})+(F_{3i}+qF_{2i}\hat{\theta})+D_3G_{3i}+qD_2G_{2i}) \\ (f_{4i}+qf_{3i})+(F_{4i}+qF_{3i}\hat{\theta})+D_4G_{4i}+qD_3G_{3i}) \end{bmatrix}\\
&+ \begin{bmatrix} F_{2i}+qF_{1i} \\ F_{3i}+qF_{2i} \\ F_{4i}+qF_{3i} \end{bmatrix} + \begin{bmatrix} I & 0 & 0 \\ -qI & I & 0 \\ 0 & -qI & I \end{bmatrix} \begin{bmatrix} \mu_{1i} \\ \mu_{2i} \\ \mu_{3i} \end{bmatrix}
\end{aligned}
\tag{20}
$$

by choosing,

$$
\begin{aligned}
\begin{bmatrix} \mu_{1r} \\ \mu_{2r} \\ \mu_{3r} \end{bmatrix} &= \begin{bmatrix} I & 0 & 0 \\ -qI & I & 0 \\ 0 & -qI & I \end{bmatrix}^{-1} \begin{bmatrix} (F_qr1) \\ (F_qr2) \\ (F_qr3) \end{bmatrix} + \begin{bmatrix} e_{2r} \\ e_{3r} \\ V_r \end{bmatrix},\\
\begin{bmatrix} \mu_{1i} \\ \mu_{2i} \\ \mu_{3i} \end{bmatrix} &= \begin{bmatrix} I & 0 & 0 \\ -qI & I & 0 \\ 0 & -qI & I \end{bmatrix}^{-1} \begin{bmatrix} (F_qi1) \\ (F_qi2) \\ (F_qi3) \end{bmatrix} + \begin{bmatrix} e_{2i} \\ e_{3i} \\ V_i \end{bmatrix},
\end{aligned}
\tag{21}
$$

where
$F_qr1 = (f_{2r}+qf_{1r})+(F_{2r}+qF_{1r}\hat{\theta})+D_2G_{2r}+qD_1G_{1r}$ $F_qr2 =$

$(f_{3r}+qf_{2r})+(F_{3r}+qF_{2r}\hat{\theta})+D_3G_{3r}+qD_2G_{2r}$ $F_qr3=(f_{4r}+qf_{3r})+(F_{4r}+qF_{3r}\hat{\theta})+D_4G_{4r}+qD_3G_{3r}$
$F_qi1=(f_{2i}+qf_{1i})+(F_{2i}+qF_{1i}\hat{\theta})+D_2G_{2i}+qD_1G_{1i}$ $F_qi2=(f_{3i}+qf_{2i})+(F_{3i}+qF_{2i}\hat{\theta})+D_3G_{3i}+qD_2G_{2i}$ $F_qi3=(f_{4i}+qf_{3i})+(F_{4i}-+F_{3i}\hat{\theta})+D_4G_{4i}+qD_3G_{3i}$.

The system (20) becomes:

$$\begin{bmatrix}\dot{e}_{1r}\\ \dot{e}_{2r}\\ \dot{e}_{3r}\end{bmatrix}=\begin{bmatrix}e_{2r}\\ e_{3r}\\ V_r\end{bmatrix}+\begin{bmatrix}F_{2r}+qF_{1r}\\ F_{3r}+qF_{2r}\\ F_{4r}+qF_{3r}\end{bmatrix}\tilde{\theta},$$
$$\begin{bmatrix}\dot{e}_{1i}\\ \dot{e}_{2i}\\ \dot{e}_{3i}\end{bmatrix}=\begin{bmatrix}e_{2i}\\ e_{3i}\\ V_i\end{bmatrix}+\begin{bmatrix}F_{2i}+qF_{1i}\\ F_{3i}+qF_{2i}\\ F_{4i}+qF_{3i}\end{bmatrix}\tilde{\theta} \tag{22}$$

taking the nominal system for (22) as:

$$\begin{bmatrix}\dot{e}_{1r}\\ \dot{e}_{2r}\\ \dot{e}_{3r}\end{bmatrix}=\begin{bmatrix}e_{2r}\\ e_{3r}\\ V_{r0}\end{bmatrix},$$
$$\begin{bmatrix}\dot{e}_{1i}\\ \dot{e}_{2i}\\ \dot{e}_{3i}\end{bmatrix}=\begin{bmatrix}e_{2i}\\ e_{3i}\\ V_{i0}\end{bmatrix} \tag{23}$$

and defining the sliding surface for nominal system (23) as:

$$\sigma_{0r}=e_{1r}+2e_{2r}+e_{3r},$$
$$\sigma_{0i}=e_{1i}+2e_{2i}+e_{3i} \tag{24}$$

then the first derivative of (24) becomes as:

$$\dot{\sigma}_{0r}=\dot{e}_{1r}+2\dot{e}_{2r}+\dot{e}_{3r}=e_{2r}+2e_{3r}+v_{0r},$$
$$\dot{\sigma}_{0i}=\dot{e}_{1i}+2\dot{e}_{2i}+\dot{e}_{3i}=e_{2i}+2e_{3i}+v_{0i} \tag{25}$$

by choosing,

$$v_{0r}=-e_{2r}-2e_{3r}-k_1sign(\sigma_{0r}),\quad k_1>0,$$
$$v_{0i}=-e_{2i}-2e_{3i}-k_2sign(\sigma_{0i}),\quad k_2>0 \tag{26}$$

we have,

$$\dot{\sigma}_{0r}=-k_1\sigma_{0r}-k_1sign(\sigma_{0r}),$$
$$\dot{\sigma}_{0i}=-k_2\sigma_{0i}-k_2sign(\sigma_{0i}). \tag{27}$$

In consequence, the nominal system (24) is asymptotically stable. The sliding surface for error dynamics presented in (22) is defined as:

$$\sigma_r=\sigma_{0r}+z_r=e_{1r}+2e_{2r}+e_{3r}+z_r,$$
$$\sigma_i=\sigma_{0i}+z_i=e_{1i}+2e_{2i}+e_{3i}+z_i, \tag{28}$$

where z_r, z_i are some itegral terms computed later. Now to avert the reaching phase, take up $z_r(0)$, $z_i(0)$ such that $\sigma_r(0)=0$, $\sigma_i(0)=0$. Choosing $v_r=v_{0r}+v_{sr}$, $v_i=v_{oi}+v_i$, where, v_{0r},v_{0i} are the nominal inputs and v_{sr},v_{si} are compensator terms which will be computed later. The first derivative of (28) can be derived as:

$$\begin{aligned}\dot{\sigma}_r&=\dot{\sigma}_{0r}+\dot{z}_r=\dot{e}_{1r}+2\dot{e}_{2r}+\dot{e}_{3r}+\dot{z}_r\\&=e_{2r}+(F_{2r}+qF_{1r})\tilde{\theta}+2e_{3r}+2(F_{3r}+qF_{2r})\tilde{\theta}+(F_{4r}\\&\quad+qF_{3r})\tilde{\theta}+v_{0r}+v_{sr}+\dot{z}_r\\\dot{\sigma}_i&=\dot{\sigma}_{0i}+\dot{z}_i=\dot{e}_{1i}+2\dot{e}_{2i}+\dot{e}_{3i}+\dot{z}_i\\&=e_{2i}+(F_{2i}+qF_{1i})\tilde{\theta}+2e_{3i}+2(F_{3i}+qF_{2i})\tilde{\theta}+(F_{4i}\\&\quad+qF_{3i})\tilde{\theta}+v_{0i}+v_{si}+\dot{z}_i\end{aligned} \tag{29}$$

The Lyapunov stability function for (29) can be defined as: $V=\frac{1}{2}\sigma_r^T\sigma_r+\frac{1}{2}\sigma_i^T\sigma_i+\frac{1}{2}\tilde{\theta}^T\tilde{\theta}$. By properly defining the adaptive laws $\tilde{\theta}$, $\hat{\theta}$ and computing v_{sr}, v_{si}, it is possible to get first derivative of Lyapunov stability function as $\dot{V}<0$.

Theorem 2. For the Lyapunov equation $V=\frac{1}{2}\sigma_r^T\sigma_r+\frac{1}{2}\sigma_i^T\sigma_i+\frac{1}{2}\tilde{\theta}^T\tilde{\theta}$ it is possible to get $\dot{V}<0$ conceding that the adaptive laws $\dot{\hat{\theta}}$, $\dot{\tilde{\theta}}$ and the values of v_{sr}, v_i are chosen as:

$$\begin{aligned}&\dot{z}_r=-\dot{e}_{2r}-2e_{3r}-v_{0r},v_{sr}=-k-3\sigma_r-k_3sign(\sigma_r)\\&\dot{z}_i=-\dot{e}_{2i}-2e_{3i}-v_{0r},v_{si}=-k-4\sigma_i-k_4sign(\sigma_i)\\&\dot{\tilde{\theta}}=-\sigma_r^T\{(F_{2r}+qF_{1r})^T+2(F_{3r}+qF_{2r})^T+(F_{4r}+qF_{3r})^T\}\\&\quad-\sigma_i^T\{(F_{2i}+qF_{1i})^T+2(F_{3i}+qF_{2i})^T+(F_{4i}+qF_{3i})^T\}-K_5\tilde{\theta}\\&\dot{\hat{\theta}}=-\dot{\tilde{\theta}},k_i>0,i=1,\cdots,5.\end{aligned} \tag{30}$$

Proof. Since:

$$\begin{aligned}\dot{V}&=\sigma_r^T\dot{\sigma}_r+\sigma_i^T\dot{\sigma}_i+\tilde{\theta}^T\dot{\tilde{\theta}},\\\dot{V}&=\sigma_r^T\{e_{2r}+(F_{2r}+qF_{1r})\tilde{\theta}+2e_{3r}+2(F_{3r})+qF_{2r})\tilde{\theta}\\&\quad+(F_{4r}+qF_{3r})\tilde{\theta}+v_{0r}+v_{sr}+\dot{z}_r\}+\sigma_i^T\{e_{2i}+(F_{2i}+qF_{1i})\tilde{\theta}\\&\quad+2e_{3i}+2(F_{3i}+qF_{2i})\tilde{\theta}+(F_{4i}+qF_{3i})\tilde{\theta}+v_{0i}+v_{si}+\dot{z}\}\\&\quad+\tilde{\theta}^T\dot{\tilde{\theta}}\end{aligned} \tag{31}$$
$$\begin{aligned}\dot{V}&=\sigma_r^T\{e_{2r}+2e_{3r}+v_{0r}+v_{sr}+\dot{z}_r\}+\sigma_i^T\{e_{2i}+2e_{3i}+v_{0i}+v_{si}\\&\quad+\dot{z}_i\}+\tilde{\theta}^T[\dot{\tilde{\theta}}+\sigma_r^T\{(F_{2r}+qF_{1r})^T+2(F_{3r}+qF_{2r})^T+(F_{4r}\\&\quad+qF_{3r})^T\}+\sigma_i^T\{(F_{2i}+qF_{1i})^T+2(F_{3i}+qF_{2i})^T\\&\quad+(F_{4i}+qF_{3i}^T)\}].\end{aligned}$$

By replacing the values of adaptive laws $\dot{\tilde{\theta}}$, $\dot{\hat{\theta}}$ and the values of v_{sr}, v_i proposed in (30), the above system (31) becomes:

$$\begin{aligned}\dot{V}&=-k_1\sigma_r^T\sigma_r-k_2\sigma_i^T\sigma_i-k_2\tilde{\theta}^T\tilde{\theta}-k_3\sigma_r^Tsign(\sigma_r)\\&\quad-k_4\sigma_i^Tsign(\sigma_i)<0.\end{aligned} \tag{32}$$

This shows that the designed sliding surfaces σ_r, σ_i and adaptive laws $\tilde{\theta}\to 0$; therefore, $e_{kr},e_{ki}\to 0$, $k=1,2,3,4$. The convergence of error system to zero ensures HS of coupled complex chaotic permanent magnet motors systems connected in ring topology.

6. Simulation results and discussion

Simulation results were presented by taking the following initial conditions, $x_1(0) = (1+2j, 3+6j, 5)^T$, $x_2(0) = (4-2j, 1+2j, 8)^T$, $x_3(0) = (-3+4j, -2+5j, -1)^T$, $x_4(0) = (5-5j, 4-2j, 3)^T$. Figure 3(a) displays the concurrence of both the real and imaginary parts of synchronization error dynamics e_{11r}, e_{12r}, e_{13r}, e_{11i}, e_{12i} to zero, Fig. 3(b) displays the concurrence of real as well as imaginary parts of synchronization error dynamics e_{21r}, e_{22r}, e_{23r}, e_{21i}, e_{22i} to zero, Fig. 3(c) displays the concurrence of real as well as imaginary parts of synchronization error dynamics e_{31r}, e_{32r}, e_{33r}, e_{31i}, e_{32i} to zero. Figure 4 depicts that dynamic states of all the systems are synchronized. Figure 5(a) shows the convergence of anti-synchronization error dynamics e_{11r}, e_{12r}, e_{13r}, e_{11i}, e_{12i} to zero, Fig. 5(b) shows the convergence of anti-synchronization error dynamics e_{21r}, e_{22r}, e_{23r}, e_{21i}, e_{22i} to zero, Fig. 5(c) shows the convergence of anti-synchronization error dynamics e_{31r}, e_{32r}, e_{33r}, e_{31i}, e_{32i} to zero. Anti-synchronization phenomena of all the systems connected in the ring connection is depicted in Fig. 6(a–e). From this, it is very clear that the dynamic states of second systems are anti-synchronized with the dynamic states of the first system. The states of the third system are anti-synchronized with the second system but these are synchronized with the first system due to the connection arrangement. Similarly, the states of the fourth system are anti-synchronized with the third system but are synchronized with the second system. Figure 6(f) shows that the estimated parameters $\hat{a}, \hat{b}$ converge to their true values a, b respectively.

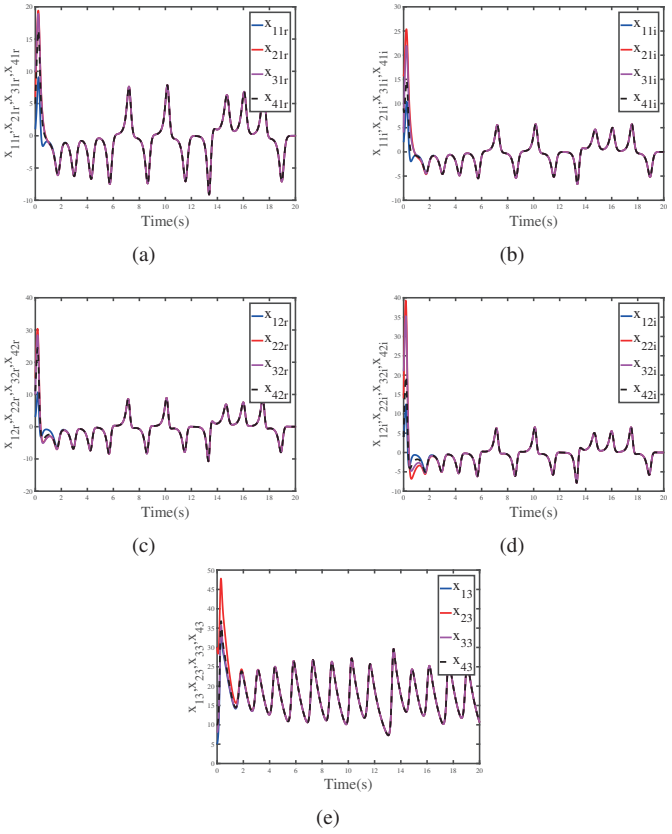

Fig. 4. (a) Synchronization of real parts of system states $x_{11r}, x_{21r}, x_{31r}, x_{41r}$, (b) Synchronization of imaginary parts of system states $x_{11i}, x_{21i}, x_{31i}, x_{41i}$, (c) Synchronization of real parts of system states $x_{12r}, x_{22r}, x_{32r}, x_{42r}$,(d) Synchronization of imaginary parts of system states $x_{12i}, x_{22i}, x_{32i}, x_{42i}$,(e) Synchronization of system states $x_{13}, x_{23}, x_{33}, x_{43}$

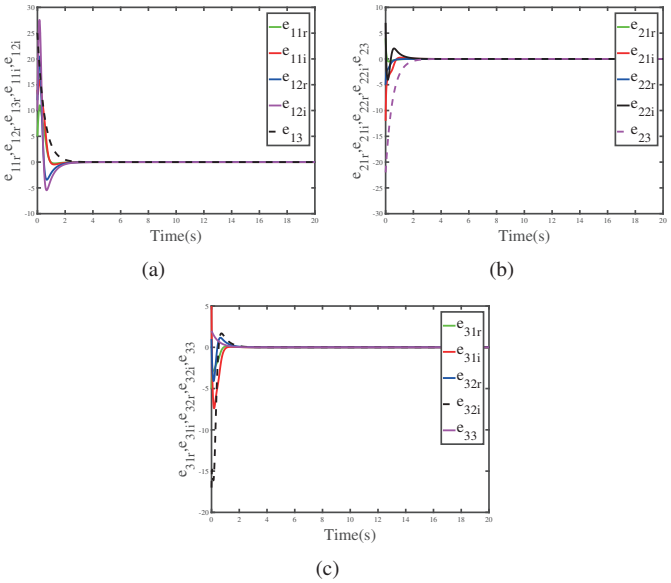

Fig. 3. Convergence of real as well as imaginary parts of synchronization error dynamics $e_{11r}, e_{12r}, e_{13r}, e_{11i}, e_{12i}$, (b) Convergence of real as well as imaginary parts of synchronization errors $e_{21r}, e_{22r}, e_{23r}, e_{21i}, e_{22i}$, (c) Convergence of real as well as imaginary parts of synchronization errors $e_{31r}, e_{32r}, e_{33r}, e_{31i}, e_{32i}$

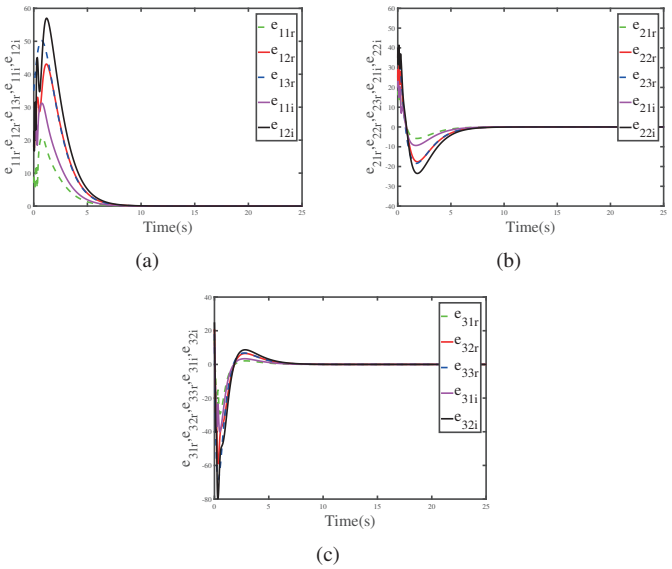

Fig. 5. (a) Convergence of real and imaginary parts of anti-synchronization errors $e_{11r}, e_{12r}, e_{13r}, e_{11i}, e_{12i}$, (b) Convergence of real and imaginary parts of anti-synchronization errors $e_{21r}, e_{22r}, e_{23r}, e_{21i}, e_{22i}$, (c) Convergence of real and imaginary parts of anti-synchronization errors $e_{31r}, e_{32r}, e_{33r}, e_{31i}, e_{32i}$

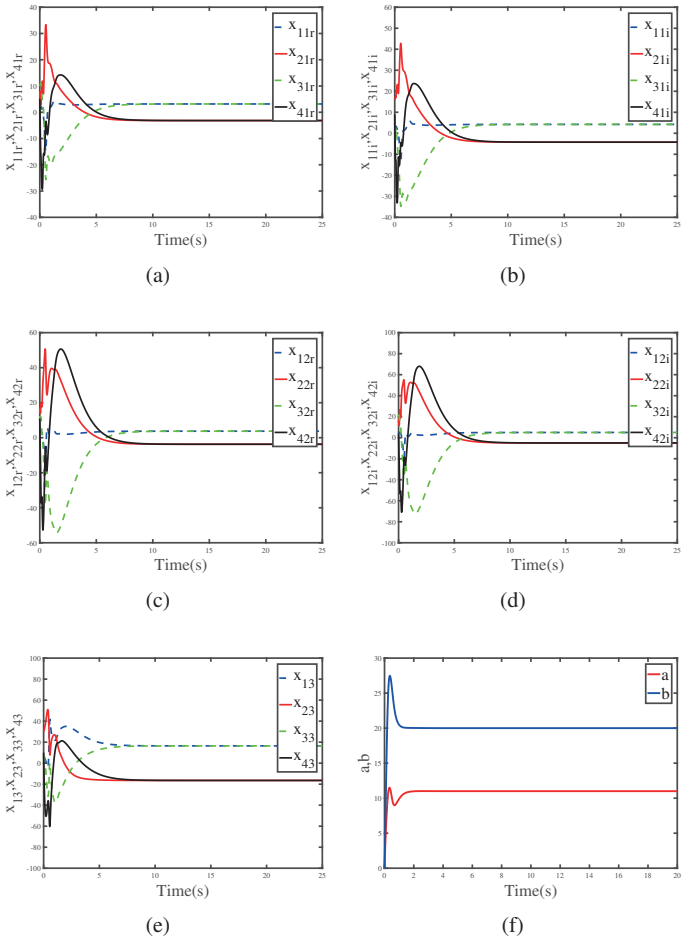

Fig. 6. (a) Anti-synchronization of real parts of system states x_{11r}, x_{21r}, x_{31r}, x_{41r}, (b) Anti-synchronization of real parts of system states x_{12r}, x_{22r}, x_{32r}, x_{42r}, (c) Anti-synchronization of real parts of system states x_{13}, x_{23}, x_{33}, x_{43}, (d) Anti-synchronization of imaginary parts of system states x_{11i}, x_{21i}, x_{31i}, x_{41i}, (e) Anti-synchronization of imaginary parts of system states x_{12i}, x_{22i}, x_{32i}, x_{42i}, (f) Convergence of estimated parameters $\hat{a}$, $\hat{b}$ to their true values a, b

7. Conclusion

The synchronization of complex chaotic PMSM systems is of increased practical importance in the field of electrical engineering. This article presents the control design method for HS and parameter identification of ring-connected complex permanent magnet synchronous motor (PMSM) systems. Design of the desired control law is a challenging task for control engineering applications due to parametric uncertainties and chaotic response to some specific parameter values. In order to achieve HS and to estimate the unknown parameters for complex PMSM systems, an adaptive integral sliding mode control is proposed. To apply adaptive ISMC, the error system is firstly converted to a unique system, consisting of nominal part together with some unknown terms which are computed adaptively. The stabilizing controller incorporating nominal control and compensator control is designed for the error system. On the other hand, the compensation controller and the adapted laws are designed to get the first derivative of the Lyapunov equation strictly negative. Simulation results verify the appropriatness of the proposed technique by showing the convergence of error dynamics to zero and HS of system states. Moreover, this work can be extended further by incorporating coupling delays.

References

[1] A.C. Fowler, J.D. Gibbon, and M.J. McGuinness, "The complex Lorenz equations", *Physica D* 4, 139–163 (1982).

[2] P. Liu, H. Song, and X. Li, "Observe-based projective synchronization of chaotic complex modified Van Der Pol-Duffing oscillator with application to secure communication", *J. Comput. Nonlinear Dyn*. 10, 051015 (2015).

[3] G.M. Mahmoud and A.A. Shaban, "On periodic solutions of parametrically excited complex non-linear dynamical systems", *Physica A* 278(3–4), 390–404 (2000).

[4] G.M. Mahmoud and A.A. Shaban, "Periodic attractors of complex damped non-linear systems", *Int. J. Non-Linear Mech*. 35(2), 309–323 (2000).

[5] G.M. Mahmoud, "Periodic solutions of strongly non-linear Mathieu oscillators", *Int. J. Non-Linear Mech*. 32(6), 1177–1185 (1997).

[6] G.M. Mahmoud and E.E. Mahmoud, "Lag synchronization of hyperchaotic complex nonlinear systems", *Nonlinear Dynamics* 67, 1613–1622 (2012).

[7] P. Liu and S. Liu, "Anti-synchronization between different chaotic complex systems", *Phys. Scr*. 83, 065006 (2011).

[8] S. Liu and P. Liu, "Adaptive anti-synchronization of chaotic complex nonlinear systems with unknown parameters", *Nonlinear Anal.-Real World Appl*. 12, 3046–3055(2011).

[9] N. Siddique and F.U. Rehman, "Parameter Identification and Hybrid Synchronization in an Array of Coupled Chaotic Systems with Ring Connection: An Adaptive Integral Sliding Mode Approach", *Math. Probl. Eng*. 2018, 6581493 (2018).

[10] G.M. Mahmoud, E.E. Mahmoud, and A.A. Arafa, "Projective synchronization for coupled partially linear complex-variable systems with known parameters", *Math. Meth. Appl. Sci*. 40(4), 1214–1222 (2017).

[11] D.W. Qian, Y.F Xi, and S.W. Tong, "Chaos synchronization of uncertain coronary artery systems through sliding mode", *Bull. Pol. Acad. Sci. Tech. Sci*. 67(3), 455–462 (2019).

[12] G.M. Mahmoud, E.E. Mahmoud, and A.A. Arafa, "On modified time delay hyperchaotic complex Lü system", *Nonlinear Dynamics* 80(1–2), 855–869 (2015).

[13] G.M. Mahmoud, T. Bountis, M.A. Al-Kashif, and A.A. Shaban, "Dynamical properties and synchronization of complex nonlinear equations for detuned lasers", *Dynam. Syst*. 24(1), 63–79 (2009).

[14] J.-B. Hu, H. Wei, Y.-F. Feng, and X.-B. Yang, "Synchronization of fractional chaotic complex networks with delay", *Kybernetika* 55, 203–215 (2019).

[15] N.A. Almohammadi, E.O. Alzahrani, and M.M. El-Dessoky, "Combined modified function projective synchronization of different systems through adaptive control", *Arch. Control Sci*. 29, 133–146 (2019).

[16] H. Su, Z. Rong, M.Z.Q. Chen, X. Wang, G. Chen and H. Wang, "Decentralized adaptive pinning control for cluster synchronization of complex dynamical networks", *IEEE Trans. Cybern*. 43, 2182–2195 (2013).

[17] A. Khan and U. Nigar, "Sliding mode disturbance observer control based on adaptive hybrid projective compound combination synchronization in fractional-order chaotic systems", *Int. J. Control Autom. Syst*. 31, 885–899 (2020).

[18] G.M. Mahmoud, E.A. Mansour, and T.M. Abed-Elhameed, "On fractional-order hyperchaotic complex systems and their generalized function projective combination synchronization", *Optik* 130, 398–406 (2017).

[19] S. Wang, X. Wang, X. Wang, and Y. Zhou, "Adaptive generalized combination complex synchronization of uncertain real and complex nonlinear systems", *AIP Adv*. 6, 045011 (2016).

[20] J. Zhou, A. Oteafy, and N. Smaoui, "Adaptive synchronization of an uncertain complex dynamical network", *IEEE Trans. Autom. Control* 51, 652–656 (2006).

[21] X. Chen, J. Qiu, J. Cao, and H. He, "Hybrid synchronization behavior in an array of coupled chaotic systems with ring connection", *Neurocomputing* 173, 1299–1309 (2016).

[22] F. Zhang, C. Mu, X. Wang, I. Ahmed, and Y. Shu, "Solution bounds of a new complex PMSM system", *Nonlinear Dynamics* 74, 1041–1051 (2013).

[23] Y.Wang, Y. Fan, Q.Wang, and Y. Zhang, "Stabilization and synchronization of complex dynamical networks with different dynamics of nodes via decentralized controllers", *IEEE Trans. Circuits Syst. I-Regul. Pap*. 59, 1786–1795 (2012).

[24] L. Zarour, K. Abed, M. Hacil, and A Borni, "Control and optimisation of photovoltaic water pumping system using sliding mode", *Bull. Pol. Acad. Sci. Tech. Sci*. 67(3), 605–611 (2019).

[25] N. Siddique, F.U. Rehman, M. Wasif, W. Abbasi, and Q. Khan, "Parameter Estimation and Synchronization of Vaidyanathan Hyperjerk Hyper-Chaotic System via Integral Sliding Mode Control", *2018 AEIT Conference IEEE*, 1–5 (2018).

[26] K. Urbanski, "A new sensorless speed control structure for PMSM using reference model", *Bull. Pol. Acad. Sci. Tech. Sci*. 65(4), 489–496 (2017).

[27] X. Sun, Z. Shi, Y. Zhou, W. Zebin, S. Wang,B. Su, L. Chen, and K. Li, "Digital control system design for bearingless permanent magnet synchronous motors", *Bull. Pol. Acad. Sci. Tech. Sci*. 66(5), 687–698 (2018).

[28] T. Tarczewski, M. Skiwski, L.J. Niewiara, and L.M. Grzesiak, "High-performance PMSM servo-drive with constrained state feedback position controller", *Bull. Pol. Acad. Sci. Tech. Sci*. 66(1), 49–58 (2018).

[29] W. Xing-Yuan and Z. Hao, "Backstepping-based lag synchronization of a complex permanent magnet synchronous motor system", *Chin. Phys. B* 22, 048902 (2013).

[30] Z. Zhang, Z. Li, M.P. Kazmierkowski, J. Rodríguez, and R. Kennel, "Robust Predictive Control of Three-Level NPC Back-to-Back Power Converter PMSG Wind Turbine Systems With Revised Predictions", *IEEE Trans. Power Electron*. 33(11), 9588– 9598 (2018).

[31] N. Hoffmann, F.W. Fuchs, M.P. Kazmierkowski, and D. Schröder, "Digital current control in a rotating reference frame – Part I: System modeling and the discrete time-domain current controller with improved decoupling capabilities", *IEEE Trans. Power Electron*. 31(7), 5290–5305 (2016).

[32] H. Won, Y.-K. Hong, M. Choi, H.-s. Yoon, S. Li and T. Haskew, "Novel Efficiency-shifting Radial-Axial Hybrid Interior Permanent Magnet Sychronous Motor for Electric Vehicle", *2020 IEEE Energy Conversion Congress and Exposition (ECCE)*, Detroit, USA, 2020, pp. 47–52.

[33] C. Jiang and S. Liu, "Synchronization and Antisynchronization of-Coupled Complex Permanent Magnet Synchronous Motor Systems with Ring Connection", *Complexity* 4, 1–15 (2017).

[34] M. Karabacak and H.I. Eskikurt, "Speed and current regulation of a permanent magnet synchronous motor via nonlinear and adaptive backstepping control", *Math. Comput. Model*. 53, 2015–2030 (2011).